KATILARIN ELEKTRONİK YAPISININ BENZETİŞİMİ

Elektronik Bant Yapıları

Doç.Dr. Yeşim Moğulkoç

E-posta: mogulkoc@eng.ankara.edu.tr
Tel: 0312 2033550

Hafta	DERS İÇERİĞİ
1.	Malzeme Bilimi: Temel Kavramlar
2.	İşletim Sistemleri, Temel Linux Komutlarının Uygulamalı Öğretilmesi ve Yoğun Madde Fiziğinde Kullanılan Yazılımlar
3.	Kristal Fiziği: Temel Kavramlar-1
4.	Kristal Fiziği: Temel Kavramlar-2
5.	Katıların Bant Teorisi
6.	**Elektronik Bant Yapıları**
7.	VİZE SINAVI

Hafta	DERS İÇERİĞİ
8.	**Durum Yoğunlukları ve Fermi Yüzeyleri**
9.	Katıların Elastik Özellikleri: Elastik sabitleri, Young, Shear Modülleri..
10.	Katıların Optik Özellikleri: Dielektrik sabitleri, Yansıma, soğurma, sönüm katsayıları, kırılma indisi
11.	Katıların Titreşimsel Özellikleri: Fononlar
12.	Kristal yapının programlama yardımıyla kurulması
13.	Katının elektronik bant yapısının programlama yardımıyla çizdirilmesi
14.	FİNAL SINAVI

Treating solids

DFT has extended to not only crystaline solids but also glasses, minerals such as zeolite, polymers, DNAs, ice, and chemical solutions. Our main concern is, of course, solids. In this chapter, we will introduce electrons into a vast terrain of varying potentials in a solid and try to identify the consequences. At the end, we will have a new formulation of the KS equations in terms of Fourier coefficients and witness the formation of band structures, a very important property of solids. To reach that end, however, two obvious issues have to be resolved: the number of electrons becomes infinite, and so does the number of atoms in solids.

We will first eliminate a large number of electrons from calculation by the pseudopotential (PP) approach. Next, we will see how the data from a small number of atoms become physically relevant to real material, using the periodic nature of solids. Two schemes will be involved in this maneuver: the periodic boundary conditions (PBC) and the supercell approach. The size of the system for calculation will be further reduced and transferred to the reciprocal lattice by the use of Brillouin zone (BZ) construction and $\boldsymbol{k}$-point sampling. Then, at the end of Sections 6.1 and 6.2, our problem for the treatment of a solid will be a small task, such as handling a handful of $\boldsymbol{k}$-points.

Pseudo Potential Approach

The PP approach (Heine 1970), like the act of the pseudo-Chaplin, mimics the true characteristics of the actual potential. The key points are dividing electrons into two groups in terms of their contributing significances, effectively freezing the nucleus and the core electrons together, and pseudizing the remaining valence wave functions. This leads to a significant reduction in the number of electrons in a system to be calculated and to a much easier description and computation of the valence wave functions.

In this section, we will classify electrons in a solid and treat them differently. Then, we will follow how the PPs are generated and how they represent the true potentials effectively for the materials that may easily consist of thousands of electrons. One can often find that any manuscript involved in the generation of a PP is generally full of equations and notations, scaring us off just by looking at it. Fortunately, the subject does not belong to us but to physicists or chemists. We are just the users of PPs—hopefully intelligent users who understand the underlying concept. This section, therefore, will address only the key points of PP generation and its applications in DFT.

Freezing Core electrons

6.1.1.1 *Core electrons*

One may say that electrons in an atomic system are all the same as one another in the sense that they normally have the same mass, charge, spin-ups and downs, etc. However, their role is very much different, depending on where they are. When atoms get together to form a solid, the core electrons (normally the electrons in the inner closed shells) stick tightly to their nucleus in a deep potential well and remain unchanged under most circumstances. Like small children around their mother, the core electrons stay in that well and rarely participate in any change of the system.

In other words, they are so localized that they do not notice whether they are in an atom or in a solid, and only oscillate rapidly due to the strong Coulomb potential by nuclei. And, at the same time, they neutralize the nuclei's charges as much as –1 per electron (in the same way that small children get the mother's immediate attention and love). Thus, their contribution to bonding is minimal when isolated atoms are brought together to form a molecule or a crystal.

Valance electrons

6.1.1.2 *Valence electrons*

On the contrary, like big brothers away from their mother, the valence electrons far from their nucleus and high above the potential well are rather independent and quite active in everything. They are the ones forming bonds, being ionized, conducting electricity in metals, forming bands, and performing other atomic activities. In metals, they can even travel the whole solid almost like a PW. In covalent or ionic solids, they are not as free as PW but roughly maintain the general picture described above.

6.1.1.3 *Frozen-core approximation*

From the computational viewpoint, we may simply remove the core (nucleus plus core electrons) from the picture and deal with only the active valence electrons. This is called frozen-core approximation, which is schematically shown in Figure 6.2. The nuclear charge is now largely screened by the core electrons and has much less effect (weaker and smoother attractive force) on the valence electrons.

Note that, in this example in Figure 6.2, the calculation load is already cut by one third. It is more impressive when we go down on the periodic table. For example, the frozen-core model for Pt only accounts for 10 valence electrons ($5d^9$ and $6s^1$) out of a total of 78 electrons ($[Xe]4f^{14}5d^96s^1$). The actual benefit is much more than what these numbers indicate as we further adopt the pseudization scheme. To make the atomic system of frozen-core physically relevant and applicable in practice, several missing details and requirements have to be added.

6.1.2 *Pseudizing the valence electrons*

When a valence wave function passes by the highly localized core region, it oscillates rapidly with many wiggles to be orthogonal to the core states as schematically shown in Figure 6.3 (the upper curve with two nodes). Remember that the orthogonal criterion guarantees each wave function to be unique and independent and thus to obey the Pauli exclusion principle.

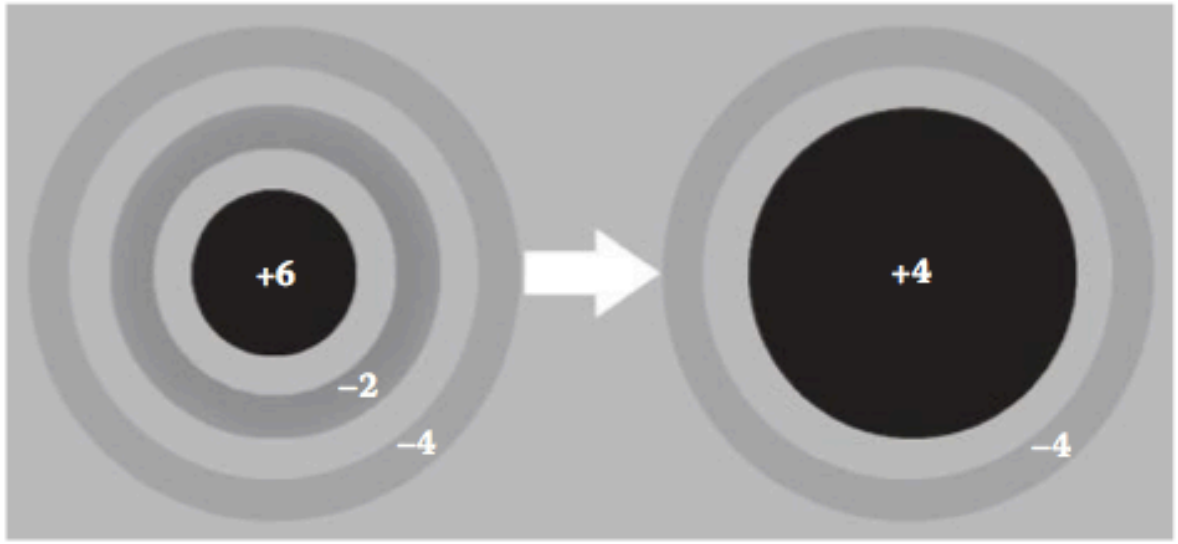

Figure 6.2 Atomic system of carbon showing the frozen core and valence electrons for the construction of a pseudopotential.

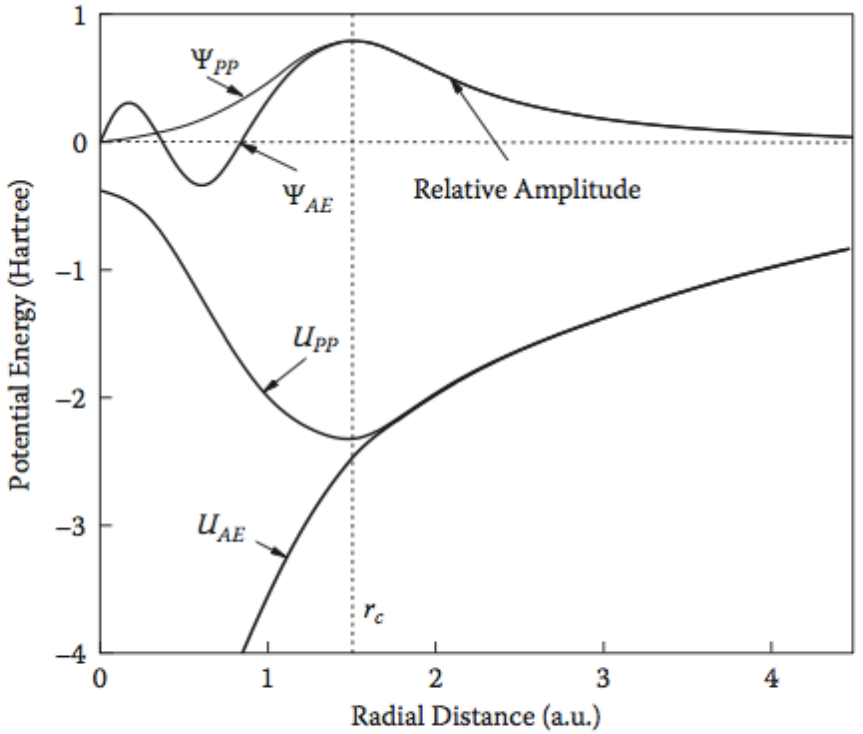

Figure 6.3 Schematic of a pseudo wave function pseudized from a 3s wave function (showing the relative amplitude in arbitrary unit) and the corresponding pseudo- and all-electron (AE) potentials.

This kind of wave function with many nodes is simply a headache. It is neither convenient to be expressed in a simple formula nor easy to be solved computationally. It would be highly appropriate if we could modulate the function to a featureless curve without any of those useless nodes. With the frozen-core approximation, the situation is just right to do that since the valence electrons are now the lowest-lying states, and there is no core electron underneath with which to be orthogonal. Thus, we can "soften" both the wave functions of the valence electrons and their potentials with ions. This procedure is specifically termed as *pseudization*.

6.1.2.1 *Pseudizing procedure*

Figure 6.3 shows an example of the all-electron (AE) and pseudized wave functions and the corresponding potentials. The standard pseudization steps are

- Select an atom as the reference state so that the formulated atomic PP can have both transferable and additive properties in application to different environments or many-atom systems.
- Calculate the exact AE potential, wave function, and energy by the DFT calculation with the use of the convenient spherical symmetry of atom; perform a precalculation for the core electrons and keep them frozen for the rest of the calculations.

- Choose a proper r_c of the atom and make the core part ($r < r_c$) of the wave function nodeless and smoother.
- At $r = r_c$, make the first and second derivatives of pseudo- and AE wave functions equal to ensure right scattering characteristics for incoming waves under the different atomic environments.
- At $r > r_c$, make the pseudo and AE wave functions exactly the same since the AE wave function in this part largely decides the behavior of the atom.
- Make the eigenvalues (energies) of the smooth pseudo and original AE wave functions the same.
- Generate a PP from the pseudo wave function and the valence electron density, and parameterize it in spherical Bessel or Gaussian functions for immediate use.

6.1.2.2 *Benefits*

In addition to the immediate benefit of removing the core electrons from calculation, other benefits are also recognized:

- The number of PWs needed for the expansion of a pseudo wave function is markedly reduced, and the calculations becomes much faster accordingly (see Section 6.4). When the DFT is armed with a PP and orbitals expanded with PWs, it becomes powerful enough to deal with thousands of electrons and opens up a wide range of problems to first-principles calculation.
- Since we normally calculate energy changes about 0.1–1.0 eV per system in a typical DFT run, any energy change calculated by DFT becomes more noticeable since a large portion of the unchanging energy is taken out as the core energy from calculation. For example, aluminum (Al) has a core potential of about –1,700 eV that will be removed by pseudization, and a valence ($3s^2$ and $3p^1$ electrons) potential of about –10 eV will remain and is subjected to change.
- The errors involved by using PPs are normally less than a couple of percentages.

- The PP approach eliminates the relativistic effect from the system since the core electrons in heavier atoms are most prone to relativity.

After this simplification, the KS equations can be rewritten with the PP (replacing the U_{eff}) and pseudized wave functions, which leads to a different charge density:

$$\left[-\frac{1}{2}\nabla^2 + U_{pp}[\rho(\boldsymbol{r})]\right]\psi_i^{PP}(\boldsymbol{r}) = \varepsilon_i \psi_i^{PP}(\boldsymbol{r}) \tag{6.1}$$

$$\rho(\boldsymbol{r}) = \sum_i \left|\psi_i^{PP}(\boldsymbol{r})\right|^2 \tag{6.2}$$

Therefore, the wave function and the charge density at the core resister only the pseudized values.

6.1.3 *Various pseudopotentials*

In the following, three common types of PPs are briefly mentioned: norm-conserving PPs, ultrasoft PPs (USPPs), and projector-augmented wave (PAW) PPs.

6.1.3.1 *Norm-conserving PPs*

If the pseudo- and AE charge densities within the core are constructed to be equal, the type of PP is called the norm-conserving PP (Hamann, Schluter, and Chiang 1979; Troullier and Martins 1991). Many PPs are generated to meet this criterion:

$$\int_0^{r_c} \left|\psi_{PP}(\boldsymbol{r})\right|^2 d\boldsymbol{r} = \int_0^{r_c} \left|\psi_{AE}(\boldsymbol{r})\right|^2 d\boldsymbol{r} \tag{6.3}$$

With this scheme, nothing is noticed differently for the valence electrons since the net charge from the core remains the same. Compared to AE methods, however, these PPs give only the valence charge densities, not the total charge densities.

6.1.3.2 *Ultrasoft PPs*

If we forget about the norm-conserving condition and, in addition to the elimination of radial nodes, shift the peak position of a wave function further to a bigger r_c with reduced peak height, we can in fact make the pseudo wave function as flat as an upside-down bowl. The potentials so generated are called ultrasoft PPs (USPPs; Vanderbilt 1990). As will be discussed in Section 6.4, this type of pseudo wave function with reduced amplitude can be easily expanded with a smaller number of PWs (smaller cutoff energy) that gives a great benefit in computation (up to ~10 times faster). USPPs also give only valence charge densities, not total charge densities.

6.1.3.3 *PAW potentials*

Projector-augmented wave (PAW) potential may be classified as a frozen-core AE potential. This type, first proposed by Blöchl (1994) and adopted by Kresse and Joubert (1999), aims for both the efficiency of the PP and the accuracy of the AE potential. It maps both core and parts of valence wave functions with two separate descriptions as shown in Figure 6.4.

The Ψ_{inter} of the valence part is represented with the PW expansion, while the Ψ_{core} of the core part is projected on a radial grid at the atom center. After the additive augmentation of these two terms, the overlapping part, Ψ_{net}, is trimmed off to make the final wave function, Ψ_{PAW}, very close to the AE wave function:

$$\Psi_{PAW} = \Psi_{inter} + \Psi_{core} + \Psi_{net} \tag{6.4}$$

Owing to the use of Ψ_{core}, the core part is well reproduced, and many PWs become unnecessary. Thus, the PAW potential calculates results as accurate as the AE full-potential approach with much less computational effort. Note that this method returns the AE charge density of valence orbitals that cannot be obtained by other standard PPs.

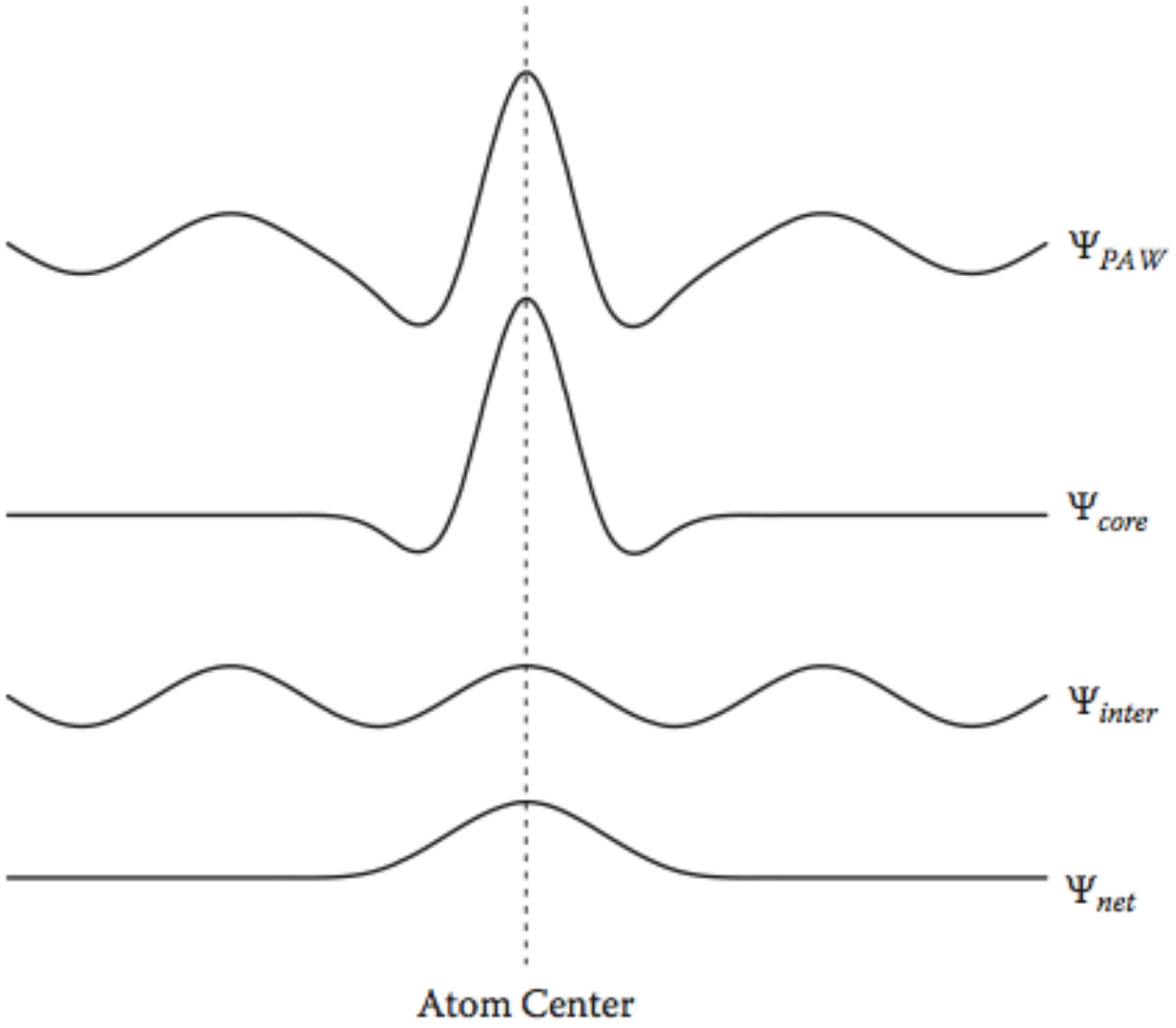

Figure 6.4 Schematic illustration of the wave components used for the construction of PAW.

6.2 *Reducing the calculation size*

Nature displays a variety of periodic events: the sun goes up and down, and the spring comes and summer follows. These temporal repetitions let us prepare for tomorrow and plan for the future. Being a part of nature, most solids are also characterized by the structural periodicity that is absent in the amorphous or liquid phase. Thus, if one crystal cell has two atoms, another one will have two atoms in the same arrangement. In the computational treatment of materials, we try to reduce the system to be calculated as small as possible, and our approach relies heavily on this periodicity of solids. The general flow along this reduction maneuver is outlined in Figure 6.5, which includes the following:

- A solid is first reduced into a supercell made of several unit cells. The constructed supercell is extended to infinity by the PBC.
- The supercell is transformed into reciprocal space and contained in a first BZ. Here, all electronic wave functions are effectively mapped with wave vector $\boldsymbol{k}$ and reciprocal lattice vector $\boldsymbol{G}$, and thus all properties are effectively represented by the Bloch equations.
- The first BZ is further reduced to a irreducible Brillouin zone (IBZ) by symmetry operations without losing any information.
- The IBZ is mapped with discrete $\boldsymbol{k}$-points, and all necessary quantities are obtained by integration/summation/extrapolation on these points.

- A solid is first reduced into a supercell made of several unit cells. The constructed supercell is extended to infinity by the PBC.
- The supercell is transformed into reciprocal space and contained in a first BZ. Here, all electronic wave functions are effectively mapped with wave vector $\boldsymbol{k}$ and reciprocal lattice vector $\boldsymbol{G}$, and thus all properties are effectively represented by the Bloch equations.
- The first BZ is further reduced to a irreducible Brillouin zone (IBZ) by symmetry operations without losing any information.
- The IBZ is mapped with discrete $\boldsymbol{k}$-points, and all necessary quantities are obtained by integration/summation/extrapolation on these points.

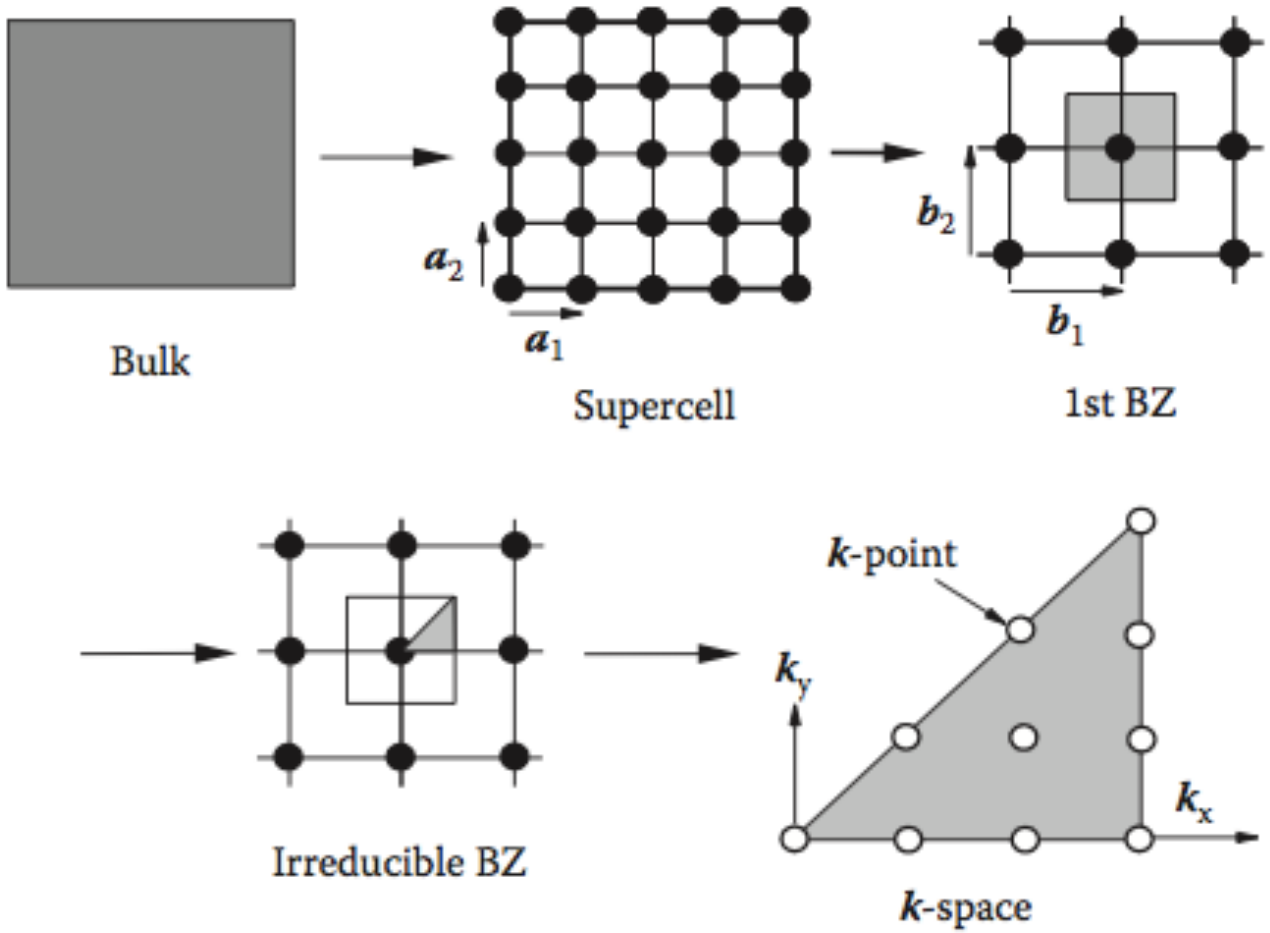

Figure 6.5 Approaches used for the treatment of solids.

6.2.1 *Supercell approach under periodic boundary conditions*

PBC was discussed in Chapter 2 when we dealt with MD, and it applies here in exactly the same way. Here, the supercell is duplicated periodically throughout the space in all directions. Therefore, even if we simulate a very small box called a supercell (several unit cells to represent the system that one intends to simulate), it can effectively represent a bulk solid. The actual calculation takes place only in the single supercell, and the remaining image supercells (26 in the nearest and more) simply copy it, which causes no significant computational cost.

If the system contains a nonperiodic entity such as a vacancy as schematically shown in Figure 6.6 in two dimensions, we can apply the same approach by including the vacancy into the supercell. Note that, however, the supercell must be sufficiently big so that we can safely assume that the interactions between the vacancy and its images in neighboring supercells are negligible.

This supercell approach under PBC can be conveniently extended to any system: bulk, atom, slab, or cluster as shown in Figure 2.10, and thus we can effectively mimic any actual solid behavior. The problem thus becomes one of solving the KS equations only within a single supercell. These imposed tricks can be used only if the supercell is neutral in charge and does not have any dipole moment. If there is any, a correction is necessary.

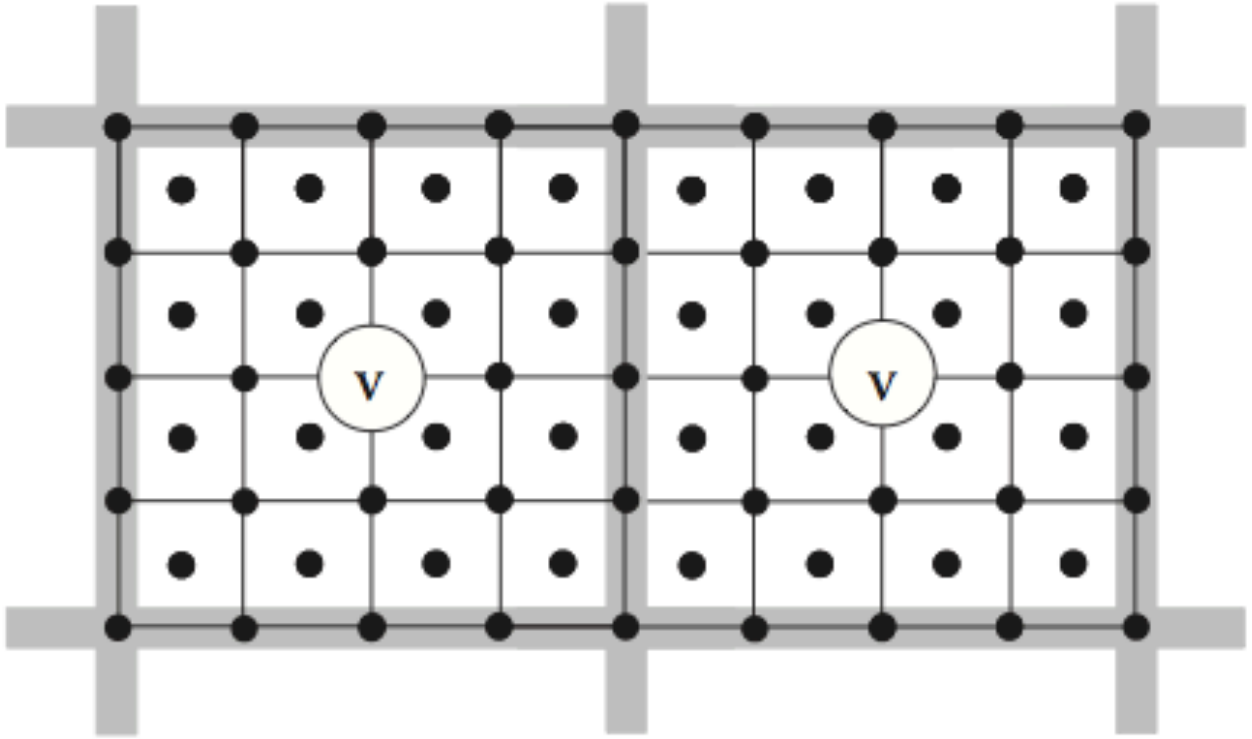

Figure 6.6 Two supercells under the periodic boundary conditions showing the interaction distance of four lattices between vacancies.

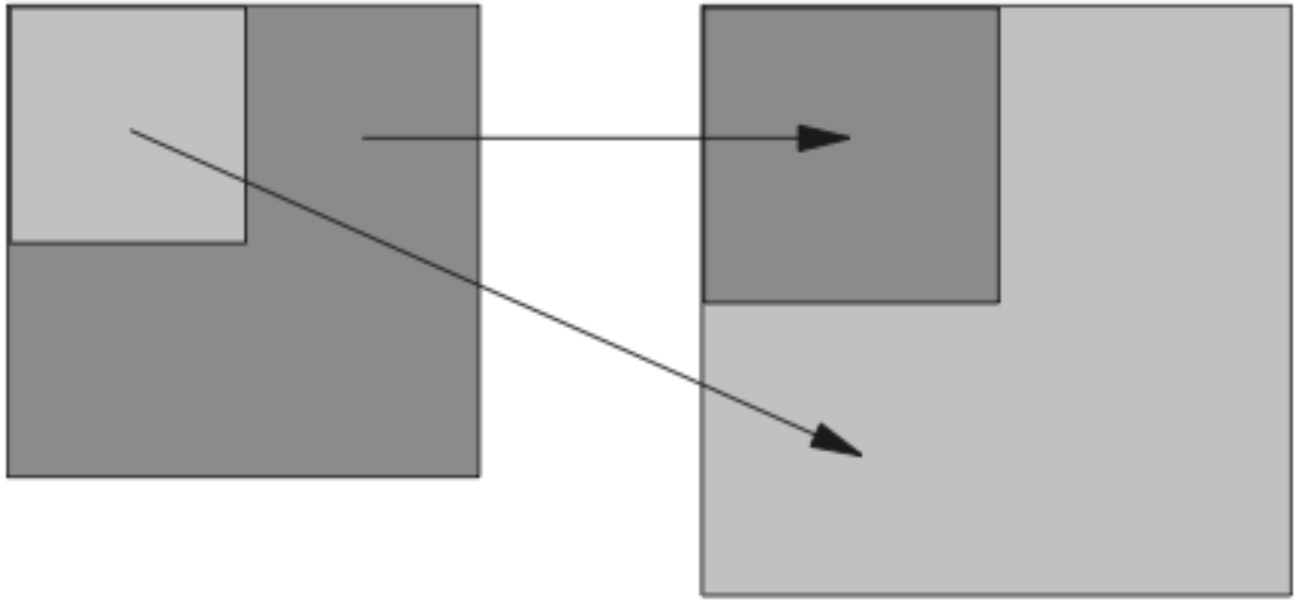

Figure 6.8 Relationship between a supercell in the real space and the corresponding reciprocal lattice in the reciprocal space in two dimensions.

6.2.2.2 *The first Brillouin zone*

Like a primitive cell in the real space, the first BZ is a primitive cell of the reciprocal lattice. In two dimensions, for example, it is constructed by the following steps (see Figure 6.10):

- Draw a reciprocal lattice.
- Draw lines from a reference lattice point to its nearest neighbors and bisect the lines perpendicularly.
- The formed square (polygon in three dimensions) with these bisecting lines is the first BZ.

The first BZ in three dimensions can be constructed similarly but is much more complicated. Taking the surfaces at the same bisecting distances

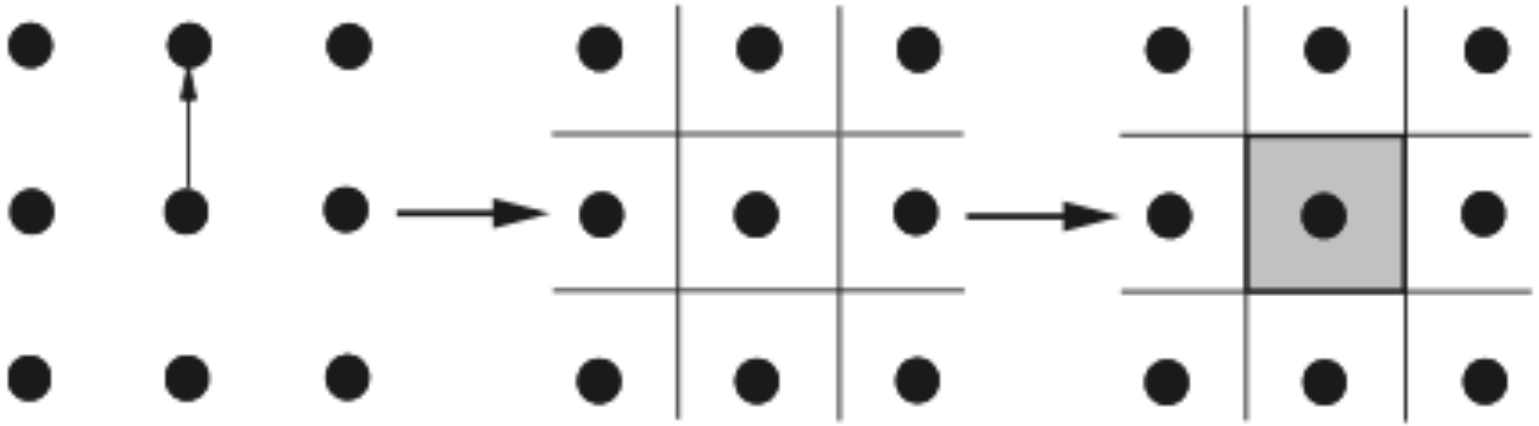

Figure 6.10 Construction steps of the 1st Brillouin zone (grey area) of two-dimensional square lattice.

from one lattice point (Γ-point) to its neighbors, the volume so formed becomes the first BZ. An example is shown in Figure 6.11 for the first BZ of an FCC lattice. It also shows some of the special points and lines of symmetry that become important when we discuss the ***k***-points later.

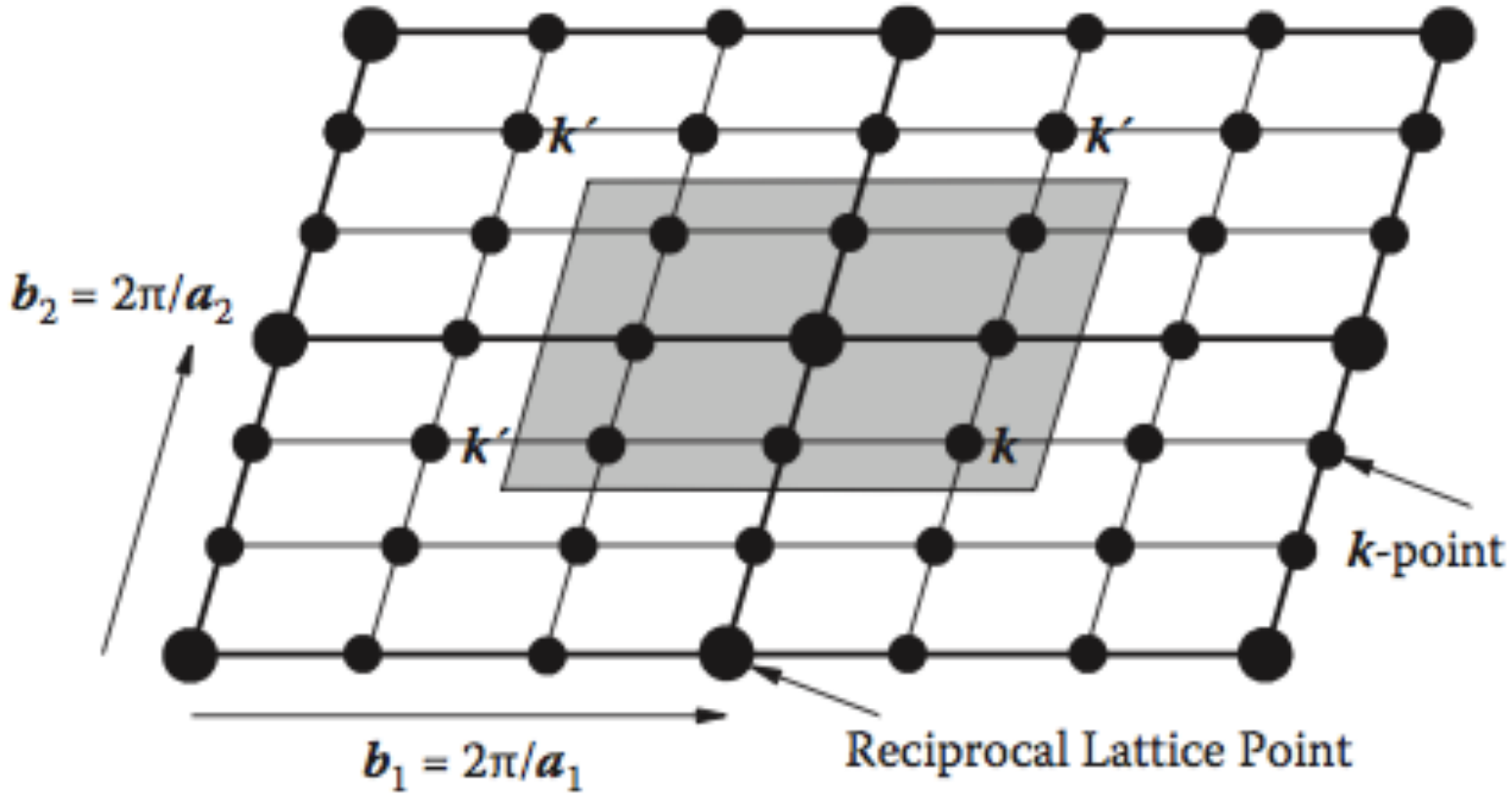

Figure 6.12 Equivalent wave vectors in the reciprocal lattice.

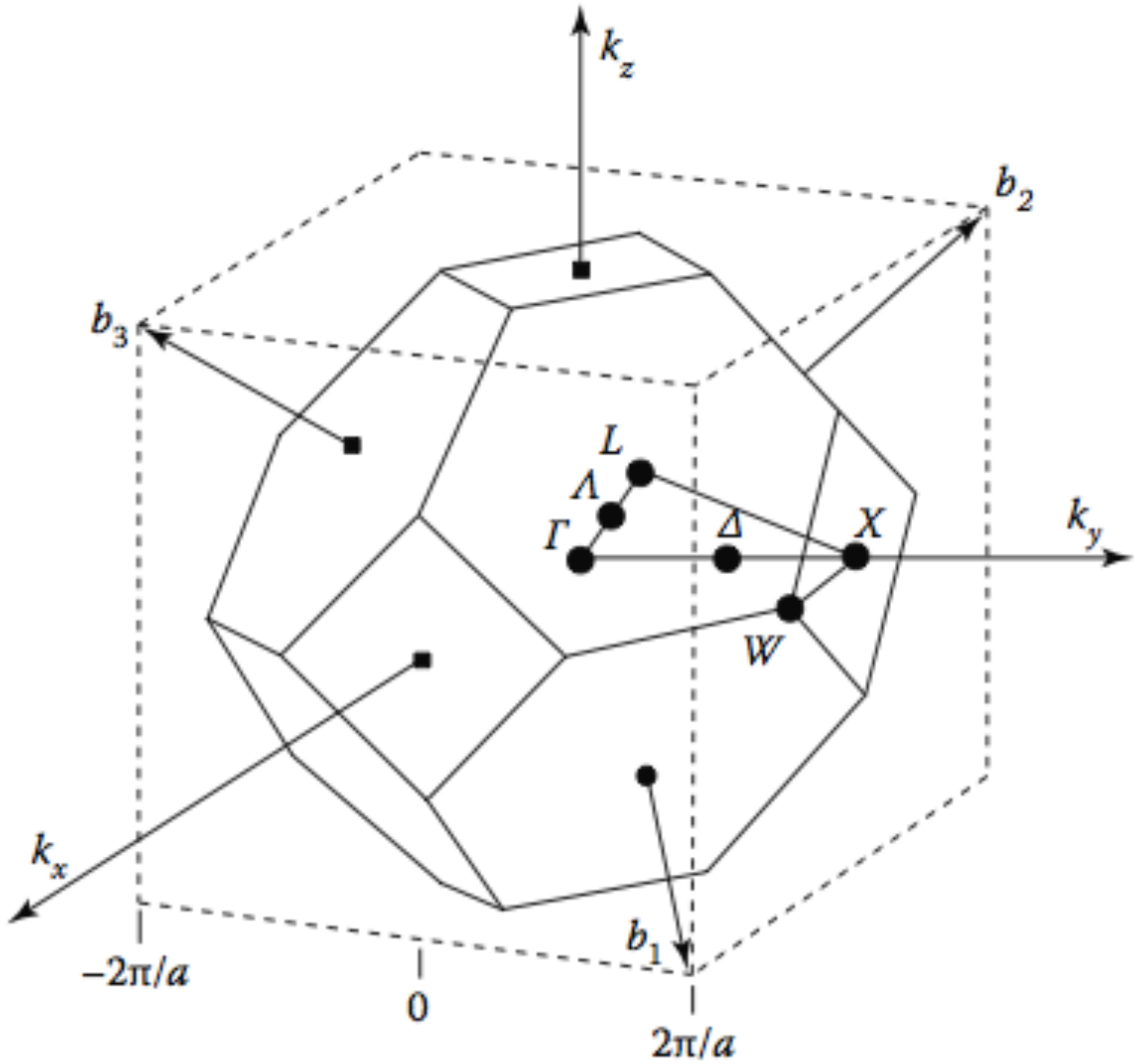

Figure 6.11 First Brillouin zone of FCC lattice showing some of the high symmetry lines and points.

6.4.3 *KS orbitals and bands*

We are now at the final stage of discussion for solids in relation to the DFT. As schematically shown in Figure 6.15, we reduced a solid into

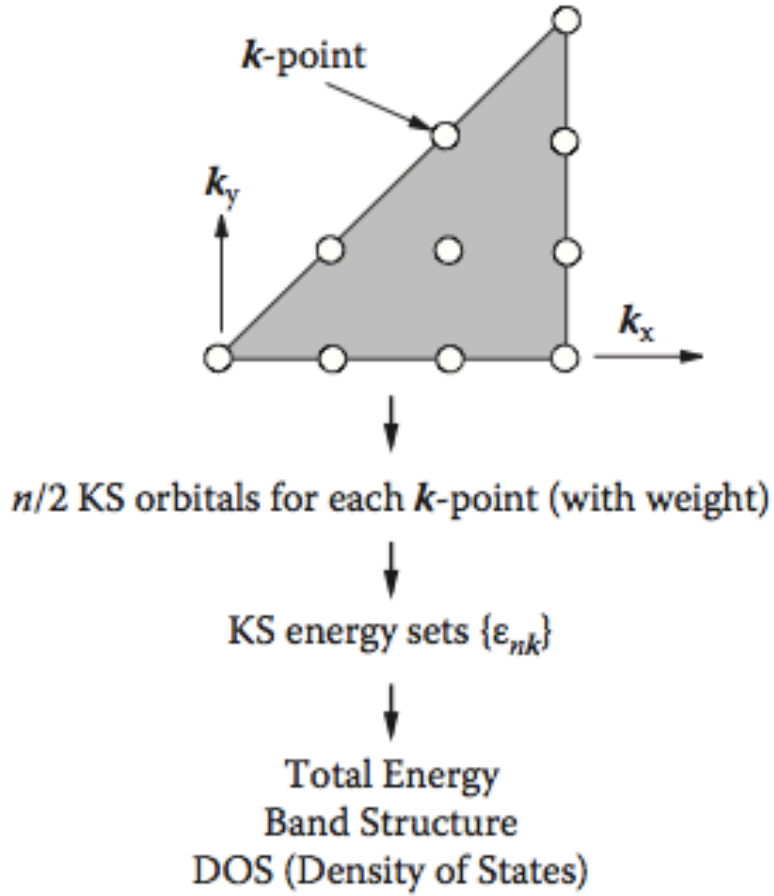

Figure 6.15 Data production from the solutions of KS equations.

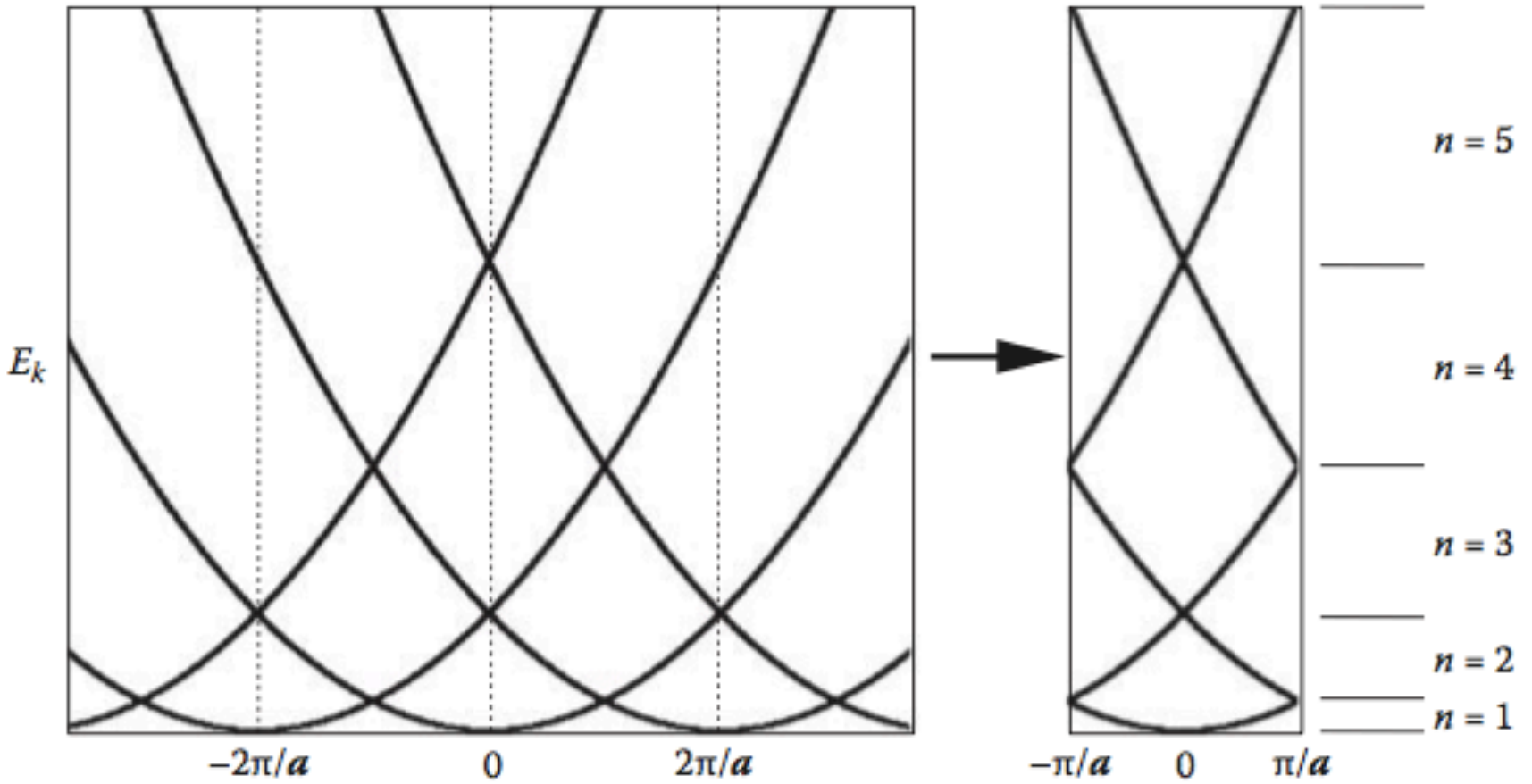

Figure 6.16 Band structures of a free-electron system showing energy curves in terms of ***k***-vector in extended (left) and reduced (right) presentations.

a wedge-shaped IBZ from which a set of KS orbital energies, $\{\varepsilon_{nk}\}$, is calculated. In this subsection, we will follow the process of electrons forming bands in solids.

6.4.3.1 *Band structure of free electron*

Let us first draw a band structure for a free electron. A free electron has only kinetic energy as given in Equation 6.25. Figure 6.16 illustrates the band structures of a free electron showing energy curves in an extended (left) and a reduced (right) presentation. Note that the energy curves are continuous without any gap and any state with $\boldsymbol{k}$ beyond the first BZ (shown up to $\pm 2\boldsymbol{G}$ in Figure 6.16) is the same to a state inside the first BZ with a different band index n.

6.4.3.2 *Band structure of electrons in solids*

The first thing happening on the electrons in solids is the formation of bands. When atoms are isolated, each electron occupies specific and discrete orbitals: 1s, 2p, 2d, etc. When they form a solid, the core electrons remain as they are, sticking to their nuclei in deep potential wells ($U \propto -1/r$). The valence electrons, however, meet each other in solids and try to occupy the same energy level. For example, in an N-atom system, there will be N 3d-orbitals trying to occupy the 3d-energy level. Eventually, they settle down by sharing the 3d-energy level together and form the energy band as shown in Figure 6.17. In this energy band, all the N energy levels from each atom are separated by almost indistinguishable differences. Among the valence bands, the band with higher energy is wider since its electrons interact more actively.

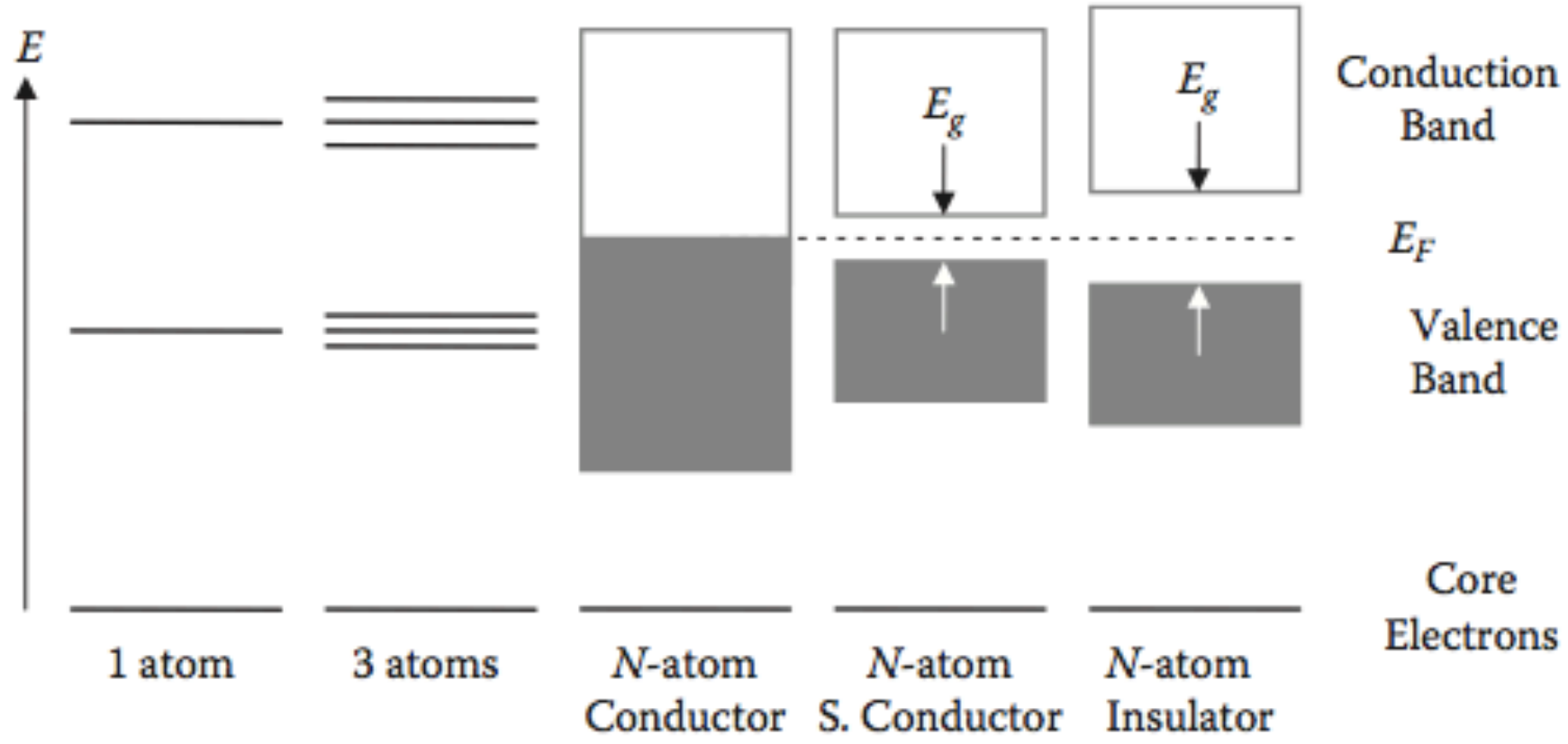

Figure 6.17 Formation of bands and band gaps when isolated atoms become various solids.

6.4.3.3 *Density of states*

The electronic structure of a solid can be characterized in another way, that is the density of states (DOS) diagram (see Chapter 7, Section 7.8). The DOS defines the number of electronic states per unit energy range. For a free electron in one-dimension, the energy relation is

$$\varepsilon_k = \frac{\hbar^2}{2m} k^2 \tag{6.33}$$

And, the total number of states, $n(\varepsilon)$, is

$$n(\varepsilon) = \frac{V}{3\pi^2} k_F^3 = \frac{V}{3\pi^2} \left(\frac{2m\varepsilon}{\hbar^2} \right)^{3/2} \tag{6.34}$$

The DOS is then

$$D(\varepsilon) = \frac{dn}{d\varepsilon} = \frac{V}{2\pi^2} \left(\frac{2m}{\hbar^2} \right)^{3/2} \varepsilon^{1/2} \propto \sqrt{\varepsilon} \tag{6.35}$$

The DOS of a free-electron system at 0 K is illustrated in Figure 6.18 as the solid curve, indicating the maximum DOS that an energy level can possibly have.

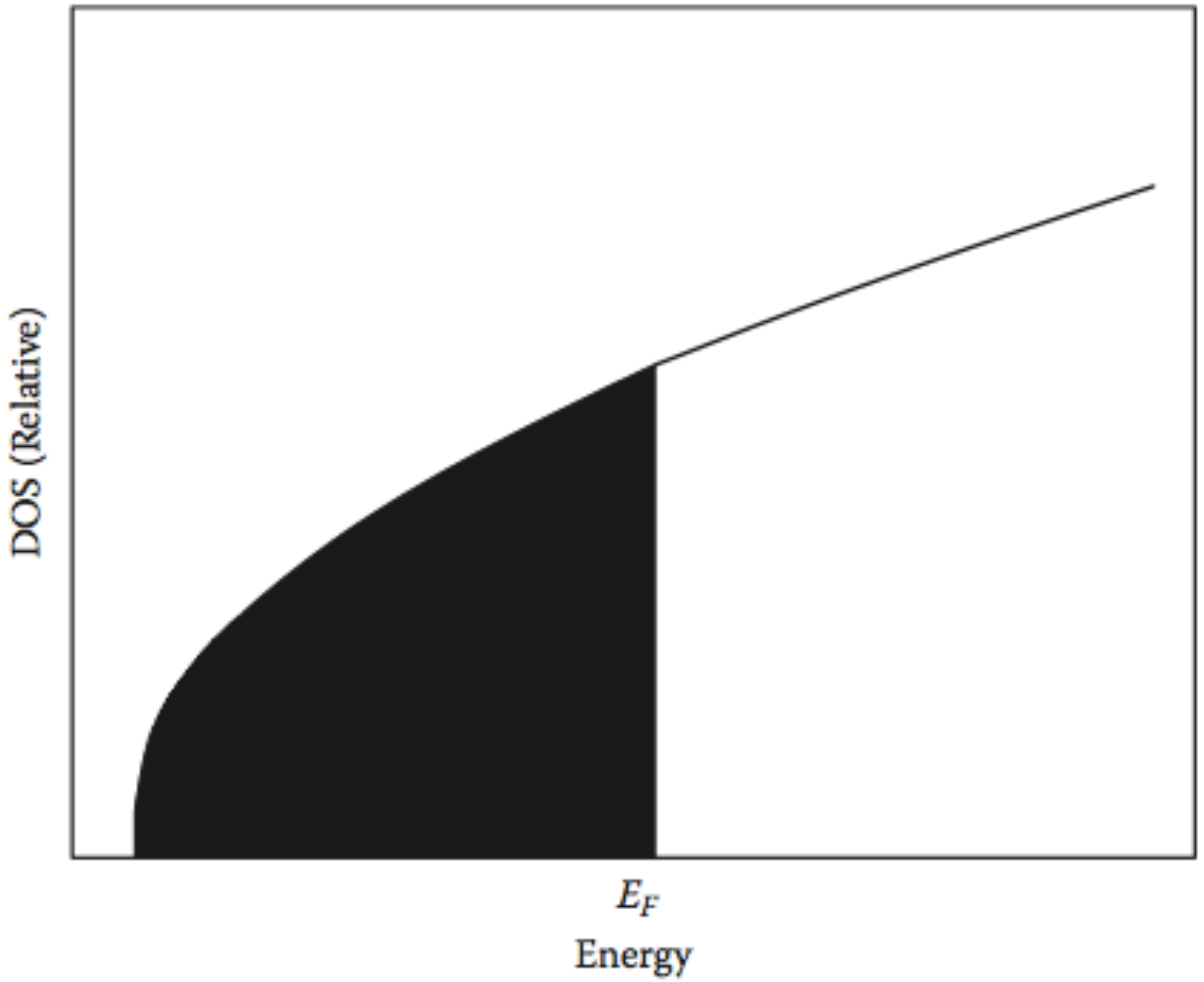

Figure 6.18 DOS of a free-electron system at 0 K. (The dark area represents occupied energy levels.)

Furthermore, the integral of DOS up to the Fermi level gives the total number of electrons in the system:

$$\int_0^{E_F} D(\varepsilon)d\varepsilon = n \tag{6.36}$$

Whether any particular state is occupied by electron or not is decided by the Fermi–Dirac distribution function, $f(\varepsilon)$ (Dirac 1926; Fermi 1926) at nonzero temperatures:

$$\int_0^{\infty} D(\varepsilon)f(\varepsilon) = n \tag{6.37}$$

At a finite temperature, there will be a change of the DOS line at the Fermi energy, that is, some electrons are thermally excited and cross over the Fermi line, changing the line to a reversed "S" curve. The actual band structure and DOS are much different from this simple case but have similar features (see Section 7.8).

6.5.2.1 *Gaussian smearing*

The Gaussian smearing method creates a finite and fictitious electronic temperature (~0.1 eV) using the Gaussian-type delta function just like heating the system up a little, and thus broadens the energy levels around the Fermi level.

6.5.2.2 *Fermi smearing*

The Fermi smearing method also creates a finite temperature using the Fermi–Dirac distribution function (Dirac 1926; Fermi 1926) and thus broadens the energy levels around the Fermi level:

$$f(\varepsilon)=\frac{1}{\exp[(\varepsilon-E_F)/k_BT]+1} \tag{6.41}$$

Here, E_F is Fermi energy, k_B is Boltzmann's constant, and T is absolute temperature. Now, eigenstates near the Fermi surface are neither full nor empty but partially filled, and singularity is removed at that point during calculation. Note that electronic thermal energy is roughly k_BT, which corresponds to about 25 meV at 300 K (see Figure 6.19).

6.5.2.3 *Methfessel–Paxton smearing*

This method as suggested by Methfessel and Paxton (1989) is one of the most widely used methods in practice with a single parameter σ. It uses step function expanded into polynomials and Gaussian function.

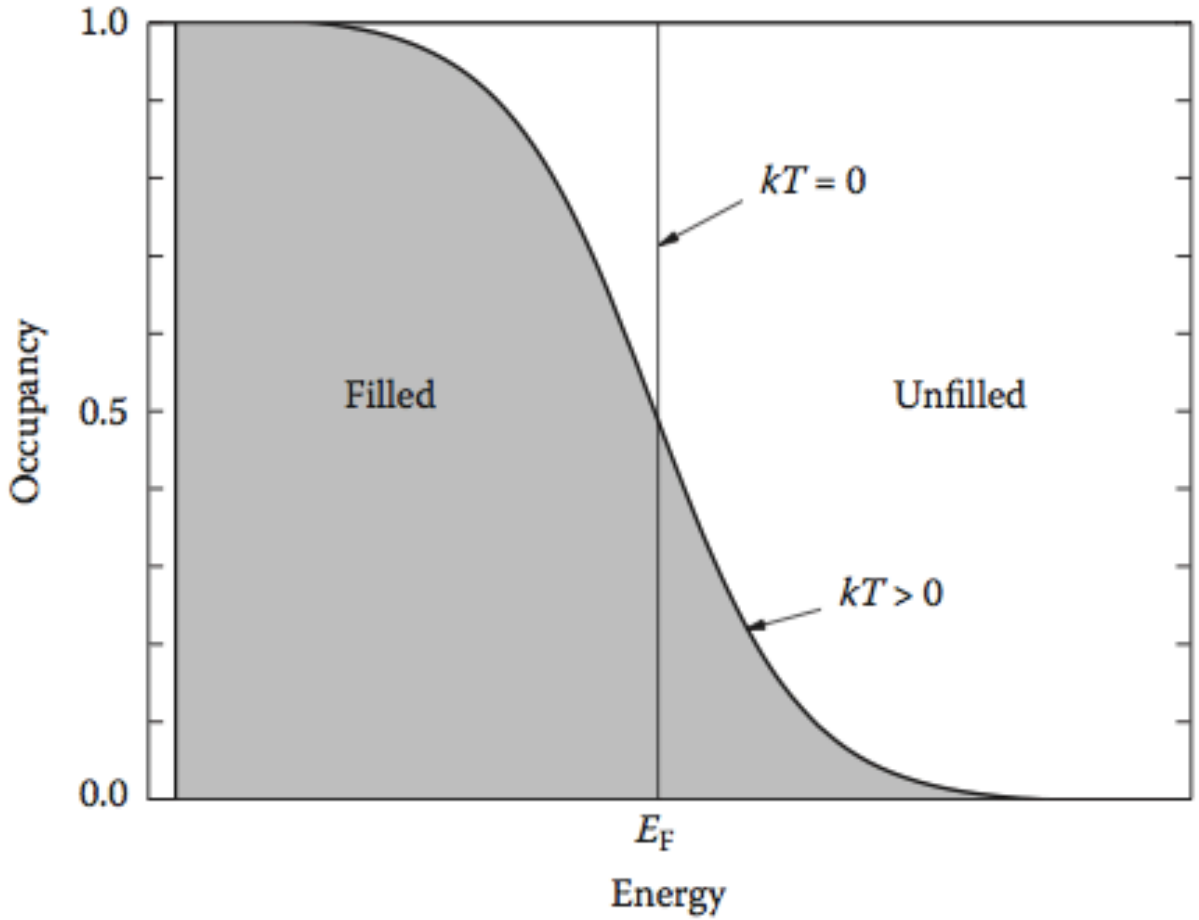

Figure 6.19 Generation of partial occupancies around the Fermi level by smearing.

6.6.2.1 *Hellmann–Feynman forces*

Forces on atoms arise from both atomic and electronic sources, and the Hellmann–Feynman theorem (Feynman 1939; Hellmann 1937) provides an efficient way to account for them, which does not require any additional effort (e.g., calculation of $\partial\phi/\partial \boldsymbol{r}_I$) other than normal electronic minimization. The theorem states that, if an exact $\hat{H}$ and the corresponding ϕ_i are calculated, the force on an atom is the expectation value of the partial derivative of $\hat{H}$ with respect to atomic position $\boldsymbol{r}_I$. Since only two potential terms are related to $\boldsymbol{r}_I$, the theorem leads to

$$\boldsymbol{F}_I = -\frac{dE}{d\boldsymbol{r}_I} = -\left\langle \phi_i \left| \frac{\partial \hat{H}}{\partial \boldsymbol{r}_I} \right| \phi_i \right\rangle = -\frac{\partial U_{IJ}}{\partial \boldsymbol{r}_I} - \int \frac{\partial U_{ext}}{\partial \boldsymbol{r}_I} \rho(\boldsymbol{r}) d\boldsymbol{r} \tag{6.43}$$